BNL-66383

Chapter 1

PION INTERFEROMETRY IN AU+AU COLLISIONS AT THE AGS

J.H. Lee
Physics Department
Brookhaven National Laboratory
Upton, NY 11973 USA
jhlee@bnl.gov

for the E866 Collaboration

Abstract Two-pion Bose-Einstein correlations have been studied using the BNL-E866 Forward Spectrometer in 11.6 A·GeV/c Au + Au collisions. The data were analyzed using three-dimensional correlation parameterizations to study transverse momentum-dependent source parameters. The freeze-out time and the duration of emission were derived from the source radii parameters.

Keywords: AGS, Au+Au, pion correlation

1. INTRODUCTION

Pion interferometry measures an enhancement at small relative momenta from Bose-Einstein symmetrizations of two identical pions, which leads to information on the space-time structure of the particle-emitting source in heavy ion collisions [1]. The dynamical nature of collisions limits the Bose-Einstein Correlation measurements to the extent of space-time "region of homogeneity" from which bosons of similar momenta are emitted. Thus correlation studies as s function of transverse momentum enable one to obtain a more complete picture of the dynamical space-time structure of the source [2].

2. EXPERIMENT

The beam of 11.6 A·GeV/c Au ions from the BNL Tandem-AGS complex was incident normally upon a Au target.

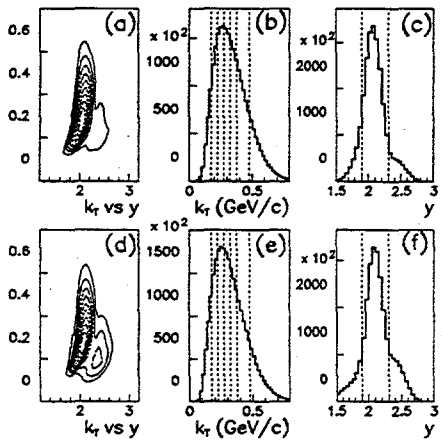

Figure 1.1 The distribution of the average transverse momentum (K_T) vs. the rapidity (y) and their projections for the $\pi^+\pi^+$ (a,b,c) and $\pi^-\pi^-$ (d,e,f) pairs. The dotted lines in figures (b) and (e) represent the K_T bins, and the dotted lines in figures (c) and (f) show the rapidity regions used in the analysis.

Data were taken using the E866 Forward Spectrometer [3]. which covers the forward rapidity region from 6 degrees to 28 degrees to the beam by rotation of the spectrometer. Particle momentum measurements were done with two tracking stations, each of which station consists of a TPC and drift chambers, located fore and aft of a dipole magnet. A Time-of-Flight wall was used for particle identification up to a particle momentum of 4 GeV/c for pions.

The total accumulations of analyzed $\pi^+\pi^+$, $\pi^-\pi^-$, and $\pi^+\pi^-$ pairs are 1.5×10^6, 1.5×10^6, and 2.5×10^6, respectively. The 24% of the total interaction cross section events gated by the New Multiplicity Array [4] were selected for the analysis. Fig. 1.1 shows the rapidity, y, and the average transverse momentum, K_T, distributions for $\pi^+\pi^+$ and $\pi^-\pi^-$ pairs. The K_T used for the analysis is from 0.175 GeV/c to 0.475 GeV/c in 5 bins, corresponding to $< K_T > =$ 0.2, 0.25, 0.3, 0.35, and 0.425, respectively, as displayed in Fig. 1.1. The rapidity range of pairs was limited to $1.9 \leq y_{\pi\pi} \leq 2.3$ for this analysis.

3. CORRELATION FUNCTION PARAMETERIZATION

The correlation function C_2 is defined as the ratio of the two-particle probability to the product of the single-particle probabilities for particles with momenta $\boldsymbol{p}_i$. Experimentally it is given by the normalized ratio of the number of correlated (signal) pairs S to the number of uncorrelated

DISCLAIMER

DISCLAIMER

Portions of this document may be illegible in electronic image products. Images are produced from the best available original document.

(background) pairs B:

$$C_2(\boldsymbol{q},\boldsymbol{K}) = \frac{P(\boldsymbol{p}_1,\boldsymbol{p}_2)}{P(\boldsymbol{p}_1)P(\boldsymbol{p}_2)} = \mathcal{N}\cdot\frac{S}{B\cdot w_{Coulomb}}\,, \tag{1.1}$$

where $(q_0,\boldsymbol{q}) = (E_1-E_2,\boldsymbol{p}_1-\boldsymbol{p}_2)$, $\boldsymbol{K} = \frac{\boldsymbol{p}_1+\boldsymbol{p}_2}{2}$ denote the relative and average momentum of the pair, respectively, and $\mathcal{N}$ is an overall normalization constant which holds no physical significance. The signal pairs are from the same events and the background pairs are calculated by mixing different events with the same experimental conditions. The background pairs were constructed with 20 times more statistics than the number of correlated pairs, and weighted with the Coulomb factor $w_{Coulomb}$ to remove the correlation created by the Coulomb effect in the correlated pairs.

For the three-dimensional parameterization, the data were fit with the Yano-Koonin-Potgoretskii (YKP) [5, 6] scheme which is a function of the space-time components $(R_\perp, R_\parallel, R_0)$ and the average longitudinal velocity v:

$$C_2(\boldsymbol{q},\boldsymbol{K}) = \mathcal{N}[1+\lambda e^{-R_\perp^2(\boldsymbol{K})q_\perp^2 - R_\parallel^2(\boldsymbol{K})(q_\parallel^2-q_0^2)-(R_0^2(\boldsymbol{K})+R_\parallel^2(\boldsymbol{K}))(q\cdot U(\boldsymbol{K}))^2}]. \tag{1.2}$$

Here $q_\perp = \sqrt{q_{side}^2+q_{out}^2}$ and $q_\parallel$ is the longitudinal component. The four-velocity U has only a longitudinal spatial component:

$$U(\boldsymbol{K}) = \gamma(\boldsymbol{K})(1,0,0,v(\boldsymbol{K})),\ \text{with}\ \gamma = \frac{1}{\sqrt{1-v^2}}. \tag{1.3}$$

The data have been also parameterized with the Bertsch-Pratt (BP) Cartesian decomposition [7, 8]:

$$C_2(\boldsymbol{q},\boldsymbol{K}) = \mathcal{N}[1+\lambda e^{-R_{long}^2(\boldsymbol{K})q_{long}^2 - R_{side}^2(\boldsymbol{K})q_{side}^2 - R_{out}^2(\boldsymbol{K})q_{out}^2 - 2R_{out,long}^2(\boldsymbol{K})q_{out}q_{long}}] \tag{1.4}$$

where λ is a chaoticity parameter, with λ=0 corresponding to a totally coherent and λ=1 corresponding to a totally chaotic source. The longitudinal component of $\boldsymbol{q}$, q_{long} is parallel to the beam, q_{side} is perpendicular both to the beam and to the average momentum, and q_{out} is orthogonal to q_{side} and q_{long}. The source radius parameters R_{long}, R_{side}, and R_{out} correspond to three dimensional radius parameters in the (q_{long},q_{side},q_{out}) space. The "out-longitudinal" cross term [9] $R_{out,long}^2$ is included in the function to accommodate the rotation of the q_{out}-q_{long} plane. The correlation functions, Eq. 1.2 and Eq. 1.4, are evaluated in the Longitudinally Co-Moving System (LCMS), which is the longitudinally boosted frame where the average pair momentum $\boldsymbol{K}$ has no longitudinal component, $\beta_L = 0$.

4. ANALYSIS

The final state Coulomb interaction between two pions was obtained by an iterative method which takes into account the pion source size [10] and the momentum resolution. The resolution functions were calculated from the Monte-Carlo simulations of the detector system using GEANT [11] and the data reconstruction chain. Fig. 1.2 shows Coulomb correction factors for two pions with and without the momentum resolution smearing. For comparison, the Gamov function which assumes a point-like source is also displayed in the figure. To test the quality of the Coulomb corrections, the correction functions are applied to $\pi^+\pi^-$ correlations which are dominated by the mutual Coulomb interactions for small q. It is demonstrated in Fig. 1.3 that the $\pi^+\pi^-$ correction function becomes close to unity after applying the Coulomb correction function calculated for a finite source and folded with the experimental momentum resolutions. No correction is applied for Coulomb effects between the pair and the remaining particles.

Fitting the data to the correlation functions was done by minimizing the logarithm of the likelihood function:

$$-\ln \mathcal{L} = \sum_{i}^{n} [C_i B_i - S_i \ln(C_i B_i) + \ln(S_i!)], \tag{1.5}$$

where C_i is the correlation function, S_i is the number of signal counts in the i-th three dimensional $\boldsymbol{q}$ bin, and B_i is the number of background events in the bin weighted by a Coulomb factor. The minimization is done using MINUIT [12].

The resolution factors contribute to an underestimation of the source parameters. The systematic uncertainties of the fitted radius parameter are estimated to be less than 10%. No correction for this effect has been applied to the data.

5. RESULTS

Multi-dimensional source radius parameters for the five K_T bins used in the analysis are shown in Fig. 1.4 for the YKP parameterization, and for the BP parameterization in Fig. 1.5. The regions fitted for each point are indicated by lines in the horizontal direction. The longitudinal component $R_{\parallel}$ (and also R_{long}) features a clear K_T dependence. Since the slope of the decrease is expected to grow with the expansion rate of the source [2, 13, 14, 15], it can be interpreted as an indication of a longitudinal expansion of the source before freeze-out. To quantify this systematic decrease, $R_{\parallel}$ values are fit with $R_{\parallel} \propto 1/m_T^{\alpha}$, where $m_T = \sqrt{K_T^2 + m_\pi^2}$,

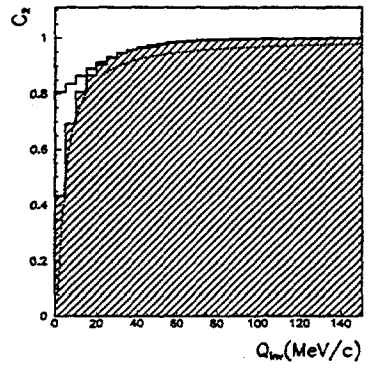

Figure 1.2 Coulomb correction functions without (shaded distribution) and with (unshaded) momentum resolution. The Gamov function is shown by the dotted curve.

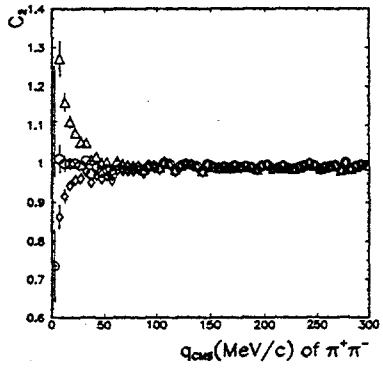

Figure 1.3 $\pi^+\pi^-$ correlation functions C_2 as a function of $|q|$ (in CMS system): The raw correlation ($\triangle$), correlations corrected with the Coulomb function ($\Diamond$) and corrected for Coulomb and momentum resolution ($\bigcirc$) are shown.

since the approximate analytic "m_T scaling" ($R_\parallel \propto 1/\sqrt{m_T}$) from the hydro-dynamical models [13, 14] has been commonly used as a basis for experimental and theoretical characterization of the dependence of the source radii on the transverse momentum. Fitted values of α for $R_\parallel$ in Fig. 1.4 are 0.75 $\pm$ 0.04 (with $\chi^2 = 1.4$) for $\pi^+\pi^+$, and 0.57 $\pm$ 0.09 ($\chi^2 = 0.29$) for $\pi^-\pi^-$, which indicates that the K_T-dependence of $R_\parallel$ is similar to or stronger than the $1/\sqrt{m_T}$ behavior. The values of $R_\perp$ show a weaker and less clear K_T-dependency compared to $R_\parallel$. Fitting $R_\perp$ to $1/m_T^\alpha$ for a quantitative comparison with $R_\parallel$ results in $\alpha = 0.26$ $\pm$ 0.07 ($\chi^2 = 0.7$) for $\pi^+\pi^+$, and 0.15 $\pm$ 0.08 ($\chi^2 = 2.0$) for $\pi^-\pi^-$. This may support the interpretation that the source undergoes some transverse expansion [15] as well as longitudinal expansion. The geometrical source parameter value $R_\perp \approx 4.5$ fm at small K_T corresponds to an r.m.s. radius of $r_{\text{r.m.s.}} = \sqrt{3}R_\perp \approx 7.8$ fm to be compared with an r.m.s. charge radius of Au nuclei measured by electron scattering [16] of 5.33 fm. The $r_{\text{r.m.s.}}$ values from the correlation measurement give larger radii than the Au r.m.s. radius. The difference can be understood as a transverse expansion contribution to the geometrical radius $R_\perp$. The source size differences between $\pi^+\pi^+$ and $\pi^-\pi^-$ are only apparent for the $R_\perp$ dimension, which qualitatively agrees with nuclear Coulomb field effects [17]. The $R_\perp$ values show a reasonable overall agreement with R_{side} within systematic uncertainties.

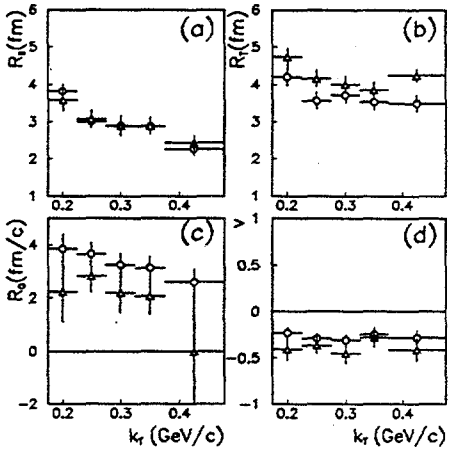

Figure 1.4 Fitted radius parameters for the YKP parameterization for $R_\parallel$ (a), $R_\perp$ (b), R_0 (c), and v (d). Circles (○) are shown for $\pi^+\pi^+$ and triangles (△) for $\pi^-\pi^-$. The error bars are statistical only.

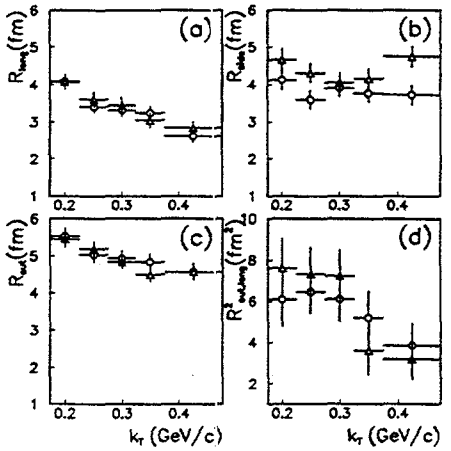

Figure 1.5 Fitted radius parameters for the BP parameterization for R_{long} (a), R_{side} (b), R_{out} (c), and $R_{out,long}$ (d). Circles (○) are shown for $\pi^+\pi^+$ and triangles (△) for $\pi^-\pi^-$. The error bars are statistical only.

One can derive an estimate of the approximate average freeze-out time τ_0 by assuming a purely longitudinally expanding system without transverse flow from [13, 14]:

$$R_\parallel = \tau_0 \sqrt{\frac{T}{m_T}}, \tag{1.6}$$

where T is a freeze-out temperature. By assuming [18] $T = 130$ MeV, the freeze-out time is $\tau_0 \approx 5$ fm/c at $< K_T > = 200$ MeV/c, and $\tau_0 \approx 4.5$ fm/c at $< K_T > = 400$ MeV/c.

An estimate of the duration of the freeze-out, $\delta\tau$ can be provided by the temporal parameter R_0, or can be obtained [19] from the difference of R^2_{out} and R^2_{side} from the BP parameterization,

$$\delta\tau = \frac{1}{\beta_\perp}\sqrt{R^2_{out} - R^2_{side}}, \tag{1.7}$$

where $\beta_\perp$ is the transverse velocity of the pair. The duration of emission given by both parameterizations are $\delta\tau \approx 2 - 4$ fm/c showing $\delta\tau \lesssim R_\perp$. This result excludes the possibility of a long-lived state created from a phase transition [20] at the AGS energy. It is shown that the $\delta\tau$ values for $\pi^+\pi^+$ are larger than for $\pi^-\pi^-$, and they increase at small K_T for both $\pi^+\pi^+$ and $\pi^-\pi^-$. Those systematic features of the effective

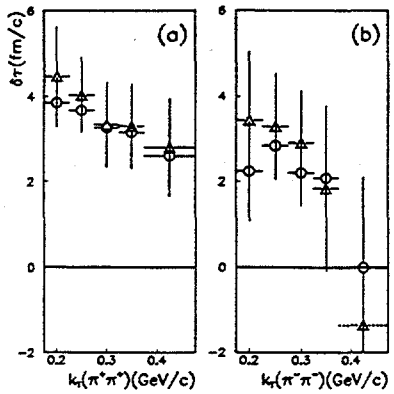

Figure 1.6 $\delta\tau$ calculated from the BP parameterization and YKP parameterizations for $\pi^+\pi^+$ (a) and $\pi^-\pi^-$ (b) as functions of K_T are shown with triangles (Δ). The last point (dotted line) in the (b) panel has $R_{side} > R_{out}$: thus an absolute value was taken for the square root in Eq. 1.7. For a comparison, R_0 values from YKP parameterization are also shown in the figures with circles ($\bigcirc$).

lifetime are consistent with both parameterizations within the systematic uncertainties as shown in Fig. 1.6.

6. SUMMARY

Preliminary results on the transverse momentum-dependent source size measurement for $\pi^+\pi^+$ and $\pi^-\pi^-$ in Au+Au collisions using the E866 Forward Spectrometer at the AGS have been presented. Multidimensional Bose-Einstein correlation functions parameterized by the Yano-Koonin-Potgoretskii method show a rapid decrease of $R_{\parallel}$ and a slower and less clear decrease of $R_{\perp}$ as the transverse momentum increases. This may indicate a strong longitudinal and a moderate transverse expansion before freeze-out. An approximate freeze-out time was estimated as $\tau_0 \approx 4.5 - 5$ fm/c with the duration of emission $\delta\tau \approx 2 - 4$ fm/c. These results agree with a Bertsch-Pratt parameterization within the systematic uncertainties.

Acknowledgments

This work was supported by the U.S. Department of Energy under contracts with BNL (DE-AC02-98CH10886), Columbia University (DE-FG02-86-ER40281), LLNL (W-7405-ENG-48), MIT (DE-AC02-76ER03069), UC Riverside (DE-FG03-86ER40271), and by NASA (NGR-05-003-513), under contract with the University of California, and by Ministry of Education and KOSEF in Korea, and by the Ministry of Education, Science, and Culture of Japan.

References

[1] See D.H. Boal, C.G. Gelbke, and B. Jennings, *Rev. Mod. Phys.* **62**, 553 (1990) for a review.

[2] U.A. Wiedemann, P. Scotto, and U. Heinz, *Phys. Rev.* C **53**, 918 (1996).

[3] L. Ahle *et al.*, *Phys. Rev.* C **57**, R466 (1998).

[4] L. Ahle, Ph.D. Thesis, MIT (1997).

[5] F. Yano and S. Koonin, *Phys. Lett.* B **78**, 556 (1978).

[6] S. Chapman, J.R. Nix and U. Heinz, *Phys. Rev.* C **52**, 2694 (1995).

[7] S. Pratt, *Phys. Rev.* D **33**, 1314 (1986).

[8] G. Bertsch, *Nucl. Phys.* A **498**, 173c (1989).

[9] S. Chapman, P. Scotto and U. Heinz, *Nucl. Phys.* B **52**, 2694 (1995).

[10] M. Baker *et al.*, *Nucl. Phys.* A **610**, 213c (1996).

[11] CERN Computing Division, CERN Program Library Long Writeup W5013.

[12] F. James, CERN Program Library Long Writeup D506.

[13] A.N. Makhlin and Yu.M. Sinyukov, *Z. Phys.* C **39**, 69 (1988).

[14] J. Bolz *et al.*, *Phys. Lett.* B **300**, 404 (1993).

[15] Wu Y.-F. *et al.*, *Eur. Phy. J.* C **1**, 599 (1998).

[16] M.A. Preston and R.K. Bhaduri, *Structure of the Nucleus*, p.99, Addison-Wesley, Massachusetts (1975).

[17] H.W. Barz, nucl-th/980827.

[18] J. Stachel, *Nucl. Phys.* A **610**, 509c (1996).

[19] H. Heiselberg, *Phys. Lett.* B **379**, 27 (1996).

[20] D.H. Rischke and M. Gyulassy, *Nucl. Phys.* A **608**, 479 (1996).